

**This is a self-archived version of an original article. This version may differ from the original in pagination and typographic details.**

**Author(s):** Bouchez, E.; Matea, I.; Korten, W.; Becker, F.; Blank, B.; Borcea, C.; Buta, A.; Emsallem, A.; France, G. de; Genevey, J.; Hannachi, F.; Hauschild, K.; Hürstel, A.; Coz, Y. Le; Lewitowicz, M.; Lucas, R.; Negoita, F.; Santos, F. de Oliveira; Pantelica, D.; Pinston, J.; Rahkila, Panu; Rejmund, M.; Stanoiu, M.; Theisen, Ch.

**Title:** New shape isomer in the self-conjugate nucleus  $^{72}\text{Kr}$

**Year:** 2003

**Version:** Published version

**Copyright:** ©2003 American Physical Society

**Rights:** In Copyright

**Rights url:** <http://rightsstatements.org/page/InC/1.0/?language=en>

**Please cite the original version:**

Bouchez, E., Matea, I., Korten, W., Becker, F., Blank, B., Borcea, C., Buta, A., Emsallem, A., France, G. D., Genevey, J., Hannachi, F., Hauschild, K., Hürstel, A., Coz, Y. L., Lewitowicz, M., Lucas, R., Negoita, F., Santos, F. D. O., Pantelica, D., . . . Theisen, Ch. (2003). New shape isomer in the self-conjugate nucleus  $^{72}\text{Kr}$ . *Physical Review Letters*, 90(8), Article 082502.  
<https://doi.org/10.1103/PhysRevLett.90.082502>

## New Shape Isomer in the Self-Conjugate Nucleus $^{72}\text{Kr}$

E. Bouchez,<sup>1</sup> I. Matea,<sup>2</sup> W. Korten,<sup>1</sup> F. Becker,<sup>1,2</sup> B. Blank,<sup>3</sup> C. Borcea,<sup>4</sup> A. Buta,<sup>4</sup> A. Emsallem,<sup>5</sup> G. de France,<sup>2</sup> J. Genevey,<sup>6</sup> F. Hannachi,<sup>7,3</sup> K. Hauschild,<sup>4,7</sup> A. Hürstel,<sup>1</sup> Y. Le Coz,<sup>1</sup> M. Lewitowicz,<sup>2</sup> R. Lucas,<sup>1</sup> F. Negoita,<sup>4</sup> F. de Oliveira Santos,<sup>2</sup> D. Pantelica,<sup>4</sup> J. Pinston,<sup>6</sup> P. Rahkila,<sup>8</sup> M. Rejmund,<sup>1,2</sup> M. Stanoiu,<sup>2</sup> and Ch. Theisen<sup>1</sup>

<sup>1</sup>CEA Saclay, DAPNIA/SPhN, F-91191 Gif-sur-Yvette, France

<sup>2</sup>GANIL, BP-5027, F-14076 Caen Cedex, France

<sup>3</sup>CEN Bordeaux-Gradignan, IN2P3-CNRS, F-33175 Gradignan Cedex, France

<sup>4</sup>IFIN-HH, P.O. Box MG6, ROM-76900 Bucarest-Magurele, Romania

<sup>5</sup>IPN Lyon, IN2P3-CNRS, F-68622 Villeurbanne Cedex, France

<sup>6</sup>ISN, IN2P3-CNRS, F-38026 Grenoble, France

<sup>7</sup>CSNSM, IN2P3-CNRS, F-91405 Orsay Cedex, France

<sup>8</sup>Department of Physics, University of Jyväskylä, P.O. Box 35, Fin-40014 Jyväskylä, Finland

(Received 21 October 2002; published 27 February 2003)

A new isomeric  $0^+$  state was identified as the first excited state in the self-conjugate ( $N = Z$ ) nucleus  $^{72}\text{Kr}$ . By combining for the first time conversion-electron and gamma-ray spectroscopy with the production of metastable states in high-energy fragmentation, the electric-monopole decay of the new isomer to the ground state was established. The new  $0^+$  state is understood as the band head of the known prolate rotational structure, which strongly supports the interpretation that  $^{72}\text{Kr}$  is one of the rare nuclei having an oblate-deformed ground state. This observation gives in fact the first evidence for a shape isomer in a  $N = Z$  nucleus.

DOI: 10.1103/PhysRevLett.90.082502

PACS numbers: 21.10.Tg, 23.20.Nx, 25.70.Mn, 27.50.+e

The shape of an atomic nucleus is governed by a delicate interplay between macroscopic effects, i.e., the response of the nuclear fluid to shape changes, and microscopic effects as given by the shell structure of the nucleon orbitals. Nuclei with closed proton and neutron shells are always spherical in their ground state, but nuclei with open shells can exhibit nonspherical equilibrium shapes. The most important deviation from sphericity is that of a quadrupole type observed for many ground states of nuclei with open shells. To first order, the binding energy should be independent of the sign of the quadrupole deformation parameter, and compressed ellipsoidal shapes (oblate nuclei) should be as equally probable as elongated ellipsoidal shapes (prolate nuclei).

In real nuclei, a prolate ground-state deformation is found to be much more abundant than oblate deformation. This finding can be related to macroscopic as well as microscopic effects. In the liquid-drop energy of prolate states, higher-order terms in the multipole expansion (including odd powers) can (partially) account for a stronger binding [1]. For realistic nuclear potentials both the  $l^2$  term, leading to a flat bottom of the potential well, as well as the spin-orbit term, needed in order to account for the shell structure, tend to favor prolate deformation [2]. Hence, most of our knowledge on nuclear shape polarization comes from the study of prolate nuclei. More complete information on the occurrence of oblate-deformed nuclei is clearly required in order to complete our understanding of nuclear shapes.

An area of great interest in this regard is a small island of nuclei between Se and Kr close to the  $N = Z$  line, where calculations predict oblate-deformed ground-state

shapes [3–6]. There is a general agreement that the shape evolution in these nuclei is rather complex due to pronounced shell gaps at nucleon numbers 34 and 36 (oblate), 34 and 38 (prolate), and 40 (spherical). Adding or removing a few nucleons can, therefore, have a dramatic effect on the nuclear shape. Competing prolate, oblate, and spherical shapes are even expected within one nucleus. Significant differences are, however, observed in the predicted binding energies for the different shapes and in the electromagnetic decay properties (see also the review on shape coexistence in [7]).

One of the fingerprints for shape coexistence in even-even nuclei is the observation of low-lying excited  $0^+$  states, which can be interpreted as the “ground state” of a different shape. If an excited  $0^+$  state comes close in energy to the lowest  $2^+$  state (or even below), its favored (or unique) decay mode is by an electric-monopole (E0) transition to the ground state. E0 transitions are non-radiative and can proceed either via internal conversion, i.e., the emission of atomic electrons from (inner) shells or via internal-pair creation if the decay energy is above 1.022 MeV. Experimentally, only very few nuclei below mass  $A = 100$  show a first excited  $0^+$  state, namely  $^{16}\text{O}$ ,  $^{40}\text{Ca}$ ,  $^{68}\text{Ni}$ ,  $^{72}\text{Ge}$ ,  $^{90,96}\text{Zr}$ , and  $^{98}\text{Mo}$ . Most of them have a closed proton and/or neutron shell and, consequently, the  $0^+$  state is located at high excitation energy leading to a fast E0 decay dominated by internal-pair creation. For lower excitation energies, as in  $^{98}\text{Mo}$ , for example, the E0 decay is rather slow, especially in low- $Z$  nuclei, and the excited  $0^+$  state becomes a metastable “shape isomer.”

First evidence for shape coexistence in neutron-deficient Kr isotopes was reported by Piercey *et al.* [8],

from irregularities observed at the bottom of the rotational bands, characteristic for a deformed shape. The high-spin states are believed to be prolate deformed since those are favored in excitation energy due to the larger moment of inertia for a prolate shape. The perturbation of the regular level sequence at lower spins is supposed to result from mixing with the coexisting oblate states. In order to prove the shape coexistence scenario, it is essential to find evidence for the oblate states and, in particular, for the excited  $0^+$  states.

First evidence for a  $0^+$  shape isomer in  $^{74}\text{Kr}$  was reported by Chandler *et al.* [9] and later confirmed by Becker *et al.* [10]. Here, the ground state is supposed to be prolate deformed while the isomeric  $0^+$  state is presumed to be of oblate deformation. The  $N = Z$  nucleus  $^{72}\text{Kr}$  is predicted to exhibit a quite unique case of shape coexistence. A low-lying excited  $0^+$  state of prolate shape is expected to coexist with an oblate-deformed ground state. Both states are believed to have a large deformation parameter of the order of  $|\beta| \sim 0.3\text{--}0.4$  [3,4].

We have performed a search for isomeric states in nuclei around mass  $A = 70$  close to the  $N = Z$  line by applying for the first time combined conversion-electron and  $\gamma$ -ray spectroscopy to nuclei produced in a fragmentation reaction. A 73 MeV/nucleon  $^{78}\text{Kr}$  beam delivered by the GANIL facility was fragmented on a Be target of 530  $\mu\text{m}$  effective thickness. The fully stripped fragments were separated in flight using the LISE3 magnetic spectrometer [11]. Using a primary beam intensity of  $\sim 20$  pA, the  $^{74}\text{Kr}$  ( $^{72}\text{Kr}$ ) ions were produced at an average rate of  $\sim 240(\sim 3)$  nuclei/s corresponding to a purity of 18% (0.4%). At the focal plane of the spectrometer (Fig. 1), the fragments passed through three  $\sim 300$   $\mu\text{m}$  thick silicon (Si) detectors, providing  $A$  and  $Z$  identification for each fragment by energy-loss and time-of-flight

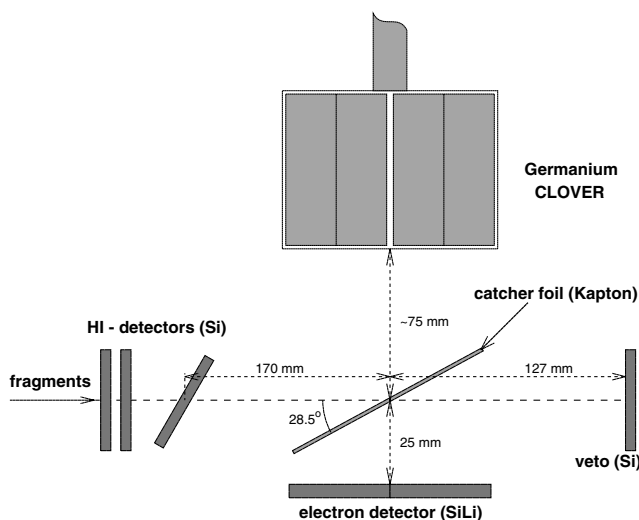


FIG. 1. Schematic view of the focal-plane detection setup. The distances are given relatively to the active surface of the detectors.

information, before being implanted into a 25  $\mu\text{m}$  thick Kapton catcher foil. The third revolving Si detector allowed one to adjust the effective matter thickness and to implant the ions of interest precisely in the last 10  $\mu\text{m}$  of the catcher foil. A final Si detector was used in order to veto other fragments that passed through the implantation foil.

The detection setup surrounding the catcher foil consisted of two segmented EXOGAM Clover Ge detectors [12], a low-energy photon detector, and a liquid-nitrogen cooled Si(Li) detector for conversion-electron detection arranged perpendicularly to the beam axis. The Si(Li) detector was shielded towards the heavy-ion Si detectors in order to prevent detection of scattered ions and  $\delta$  electrons abundantly produced during the slowing-down process. A careful determination of the detection efficiency taking into account the influence of the exact implantation point yielded absolute values of 1.1(2)% for 1.3 MeV  $\gamma$ -rays and 6.2(15)% for electrons between  $\sim 100$  keV and 2 MeV.

A spectroscopic investigation of isomers produced in projectile fragmentation is limited to states with lifetimes longer than  $\sim 100$  ns, i.e., not much shorter than the time of flight through the spectrometer. Transitions proceeding predominantly by internal conversion present a special case. Since the fragments are fully stripped of their electrons while in flight, the decay is partially blocked. In this case the time-of-flight limit applies to the much longer “apparent” lifetime of the isomeric state [13].

In Fig. 2, conversion-electron and gamma-ray spectra in coincidence with the implantation of  $^{72}\text{Kr}$  and  $^{74}\text{Kr}$  fragments are shown as obtained following the procedure described in [13]. In order to demonstrate the exceptionally clean experimental conditions, the spectra are shown on a logarithmic scale. Note also the energy threshold well below the Kr x-ray lines giving access to very low-energy transitions.

For  $^{72}\text{Kr}$ , two electron lines are observed [Fig. 2(a)] that correspond to  $K$ - and  $L$ -shell conversion of a  $671 \pm 2$  keV transition. No corresponding transition is found in the  $\gamma$ -ray spectrum (not shown) as expected for an E0 transition. This observation establishes a new  $0^+$  state as the first excited state in  $^{72}\text{Kr}$  and extends the systematics of low-lying excited  $0^+$  states in the Kr isotopes to the  $N = Z$  line. From the lifetime of the new isomer ( $\tau = 38 \pm 3$  ns), the reduced electric-monopole strength can be determined as  $\rho^2 = (72 \pm 6) \times 10^{-3}$ .

Similarly, for  $^{74}\text{Kr}$ , two electron lines are observed [Fig. 2(b)] corresponding to a 508 keV transition. Again no corresponding  $\gamma$  decay is observed, confirming our previous finding of an E0 transition at this energy [10] and assigning the corresponding  $0^+$  isomer firmly to  $^{74}\text{Kr}$ . In both cases, the  $K/L$  ratio is in accordance with the theoretical value for an E0 transition when taking into account the pile-up probability for  $K$  x-rays being detected in coincidence with a  $K$  electron. The 456 keV transition observed in the  $\gamma$ -ray spectrum associated with  $^{74}\text{Kr}$  ions

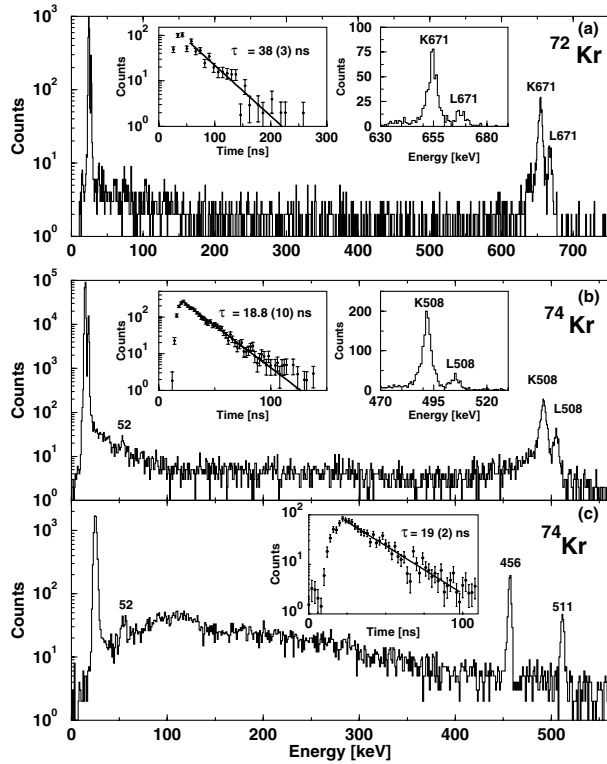


FIG. 2. Conversion-electron spectra obtained in coincidence with  $^{72}\text{Kr}$  ions (a) and  $^{74}\text{Kr}$  (b). The insets show an expansion of the region around the E0 decays and the corresponding time spectrum. (c)  $\gamma$ -ray spectrum obtained from  $^{74}\text{Kr}$  fragments including the time spectrum corresponding to the 456 keV E2 transition.

[Fig. 2(c)] corresponds to a second decay branch of the isomer through the first excited  $2^+$  state. The low-energy  $0_2^+ \rightarrow 2_1^+$  E2 transition is observed as a (very weak) line at  $\sim 52$  keV in both the Si(Li) and the Ge detectors, confirming the indirect evidence reported in [9]. We were only able to detect  $\gamma$  rays from this transition, but no conversion electrons, most likely due to the strong straggling effects in the implantation foil. From both decay branches, a new improved lifetime value of  $18.8 \pm 0.5(\text{stat}) \pm 0.5(\text{sys})$  ns is obtained.

In order to determine the E0 strength in  $^{74}\text{Kr}$ , the partial lifetime for the E0 decay has to be deduced from the E2 to E0 branching ratio  $T(\text{E}2)/T(\text{E}0)$ . The best estimate for this ratio is obtained by comparing the intensities of the E0 transition [observed in the Si(Li) detector] and the 456 keV E2 transition (observed in the Ge detectors). This results in a value of  $T(\text{E}2)/T(\text{E}0) = 1.2 \pm 0.2(\text{stat}) \pm 0.3(\text{sys})$ . The rather large systematic uncertainty is mainly related to the efficiency corrections, especially for the electrons, due to a rather strong dependence on the exact implantation point in the close geometry. This ratio is significantly larger than the one obtained in a recent beta-decay study [14], but the statistical significance of the E2 branch is much higher in our experiment. From the branching ratio a reduced E2 transition strength

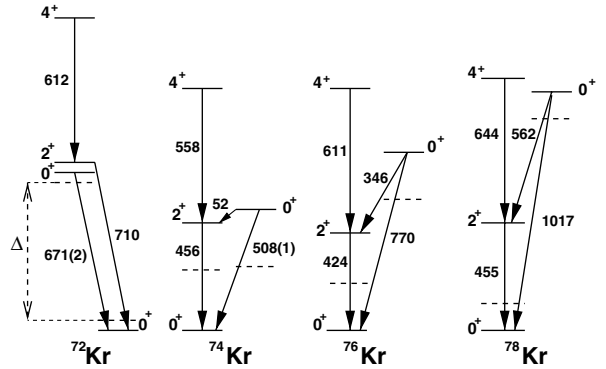


FIG. 3. Systematics of excited  $0^+$  states in neutron-deficient Kr isotopes and other low-spin states (from Refs. [15–18]). The (presumably) prolate states are shown on the left-hand side of each level scheme, while the oblate (or spherical) states are shown on the right. The position of the unperturbed  $0^+$  states (and their energy difference  $\Delta$ ) as obtained from an extrapolation procedure [8,10] are indicated as dashed lines.

of  $B(\text{E}2, 0_2^+ \rightarrow 2_1^+) = 0.56 \pm 0.23 e^2 b^2$  and a monopole strength of  $\rho^2(\text{E}0) = (85 \pm 19) \times 10^{-3}$  has been determined.

The low-spin level schemes of neutron-deficient Kr isotopes including the new excited  $0^+$  states are shown in Fig. 3. In all the isotopes, a regular rotational band, characteristic for a well-deformed shape, is observed at higher spins (not shown in Fig. 3), but for the lowest states ( $I \leq 6\hbar$ ) this regularity is lost, which is interpreted as evidence for a perturbation from other close lying states [8]. The energetic position of the unperturbed states can be obtained by an extrapolation of the rotational states towards lower spins (see [8,10]). This procedure relies on the reasonable assumption that the higher spin states are not perturbed. From the energy difference of the perturbed and unperturbed states for a given spin (denoted as  $\Delta'$  and  $\Delta$ ), the mixing matrix element ( $V$ ) and the (squared) mixing amplitudes can be derived in a two-level mixing calculation [19] (see Table I).

From the systematic behavior of the Kr isotopes, the following conclusions can be drawn. The energy of the  $0_2^+$  states follows a parabolic trend with a minimum in  $^{74}\text{Kr}$ . Here, the unperturbed states are practically degenerate

TABLE I. Results of a two-level mixing calculation [19] for the coexisting  $0^+$  states in Kr isotopes. From the energy differences of the perturbed ( $\Delta'$ ) and unperturbed ( $\Delta$ ) states, the mixing matrix element ( $V$ ) and the (squared) mixing amplitudes for the prolate ( $a^2$ ) and the oblate configuration ( $b^2 = 1 - a^2$ ) are obtained.

Nuclide	$\Delta'$ [MeV]	$\Delta$ [MeV]	$V$ [MeV]	$b^2$
$^{78}\text{Kr}$	1.01718(3)	0.80(1)	0.31(1)	0.11(2)
$^{76}\text{Kr}$	0.7700(2)	0.36(1)	0.34(1)	0.27(1)
$^{74}\text{Kr}$	0.508(1)	-0.02(1)	0.25(1)	0.52(1)
$^{72}\text{Kr}$	0.671(1)	-0.54(1)	0.20(1)	0.90(1)

( $\Delta \approx 0$ ) leading to a squared mixing amplitude of  $\sim 50\%$ , i.e., the physical states have almost the same amount of both configurations. In fact, the experimentally observed displacement of the second  $0^+$  state by 508 keV is almost entirely the result of a strong repulsion of the intrinsic states [10].

In  $^{72}\text{Kr}$ , the mixing of the  $0^+$  states is reduced again, but now the energy difference of the pure states has changed sign, i.e.,  $\Delta < 0$ , indicating that the two shapes have exchanged their relative positions. For this important conclusion, the exact location of the excited  $0^+$  state is crucial. Only the fact that the  $0_2^+$  state is located close in energy to the  $2^+$  state allows it to be identified as the prolate band head. All observations are in agreement with the theoretically expected shape change [3,4] of the ground state from being predominantly prolate in  $^{76}\text{Kr}$  to being oblate in  $^{72}\text{Kr}$ .

This scenario is also supported by the E0 strength parameters  $\rho^2$  as summarized in Table II. In the isotopes  $^{78,76}\text{Kr}$ , the decay of the excited  $0^+$  state is actually dominated by a fast high-energy E2 decay, but the much weaker E0 decay branch was also established [20]. Below mass  $A = 78$ , a very large and rather constant monopole strength is observed. The electric-monopole transition strength is related to the change in the root-mean-square charge radius of the nucleus between the initial and final states. It therefore carries important information about the change in deformation and the overlap of the wave functions. The largest E0 strength known in heavy atomic nuclei ( $\rho^2 \approx 0.1$ ) are observed for shape-coexisting states around  $A \sim 100$  [22]. The values reported here for the Kr isotopes are of very similar size.

Finally, we compare our results with the predictions from a recent Hartree-Fock-Bogoliubov (HFB) calculation [21]. It is important to note that only very few of the many calculations, which have been performed for these nuclei, concern electromagnetic transition properties, and especially the monopole strength. The experimentally observed monopole strength is larger than the values obtained in the HFB calculation ( $\rho_{\text{HFB}}^2$  in Table II), especially for  $^{74}\text{Kr}$ . The authors of Ref. [21] note that the oblate-prolate shape mixing and, hence, the monopole strength are very sensitive to small changes in specific isospin  $T = 0$  matrix elements involving the  $f_{5/2}$ ,  $f_{7/2}$ , and  $g_{9/2}$  orbitals. The new experimental results may help to understand the role of the proton-neutron interaction for the development of deformation in this mass region.

In summary, we have observed the first case of shape isomerism in a  $N = Z$  nucleus, which at the same time supports the predicted scenario of oblate-prolate shape coexistence in this mass region.  $^{72}\text{Kr}$  seems to be one of the rare nuclei with a rather pure oblate-deformed ground state. The low-energy spectra of the Kr isotopes can be understood in terms of a simple two-level mixing model. The large E0 matrix elements connecting the  $0^+$  states are consistent with a large difference in deformation and

TABLE II. Experimental E0 strength parameter  $\rho^2$  in light Kr isotopes as determined from the lifetime and the branching ratio of the  $0_2^+$  states. The experimental values for  $^{78,76}\text{Kr}$  are taken from [20] and the HFB results from [21].

Nuclide	$^{78}\text{Kr}$	$^{76}\text{Kr}$	$^{74}\text{Kr}$	$^{72}\text{Kr}$
$\tau(0_2^+)$	11(3) ps	61(9) ps	18.8(10) ns	38(3) ns
$\frac{T(E2)}{T(E0)}$	3360(150)	490(19)	1.2(5)	0
$\rho_{\text{exp}}^2$	0.047(13)	0.079(11)	0.085(19)	0.072(6)
$\rho_{\text{HFB}}^2$	...	...	$\sim 0.035$	$\sim 0.063$

should allow for a more stringent test of nuclear models. While our studies yield the strongest evidence thus far obtained in this mass region for the scenario of (strongly) interacting states with very different shapes, the experimental proof for large (intrinsic) quadrupole moments having opposite signs for the presumed oblate and prolate configurations is still missing. Coulomb excitation experiments with radioactive Kr beams from the SPIRAL facility at GANIL are currently under way in order to solve this puzzling question.

This work has been supported by the EU-IHP programme (Contract No. HPRI-CT 1999-00019).

- 
- [1] S. Freund *et al.*, Phys. Lett. B **302**, 167 (1993).
  - [2] N. Tajima and N. Suzuki, Phys. Rev. C **64**, 037301 (2001).
  - [3] R. Bengtson, in *Nuclear Structure of the Zirconium Region*, edited by J. Eberth, R. A. Meyer, and K. Sistemich (Springer, New York, 1988).
  - [4] W. Nazarewicz *et al.*, Nucl. Phys. A **435**, 397 (1985).
  - [5] P. Bonche *et al.*, Nucl. Phys. A **443**, 39 (1985).
  - [6] A. Petrovici *et al.*, Nucl. Phys. A **483**, 317 (1988); Prog. Part. Nucl. Phys. **43**, 485 (1999).
  - [7] J. L. Wood *et al.*, Phys. Rep. **215**, 101 (1992).
  - [8] R. B. Piercy *et al.*, Phys. Rev. Lett. **47**, 1514 (1981).
  - [9] C. Chandler *et al.*, Phys. Rev. C **56**, R2924 (1997); Phys. Rev. C **61**, 044309 (2000).
  - [10] F. Becker *et al.*, Eur. Phys. J. A **4**, 103 (1999).
  - [11] R. Anne and A. C. Mueller, Nucl. Instrum. Methods Phys. Res., Sect. B **70**, 276 (1992).
  - [12] S. L. Shepherd *et al.*, Nucl. Instrum. Methods Phys. Res., Sect. A **434**, 373 (1999).
  - [13] R. Grzywacz *et al.*, Phys. Lett. B **355**, 439 (1997).
  - [14] E. F. Zganjar *et al.* (to be published).
  - [15] S. M. Fischer *et al.*, Phys. Rev. Lett. **87**, 132501 (2001).
  - [16] N. S. Kelsall *et al.*, Phys. Rev. C **64**, 024309 (2001).
  - [17] D. Rudolph *et al.*, Phys. Rev. C **56**, 98 (1998).
  - [18] C. J. Gross *et al.*, Nucl. Phys. A **501**, 367 (1989).
  - [19] P. J. Brussard and P. W. M. Glaudemans, *Shell Model Applications in Nuclear Spectroscopy* (North-Holland, Amsterdam, 1977), p. 56.
  - [20] A. Giannatiempo *et al.*, Phys. Rev. C **52**, 2444 (1995); (private communication).
  - [21] A. Petrovici *et al.*, Nucl. Phys. A **665**, 333 (2000).
  - [22] J. L. Wood *et al.*, Nucl. Phys. A **651**, 323 (1999).